High-precision time-space correlation through coupled apatite and zircon tephrochronology: An example from the Permian-Triassic boundary in South China

Björn Baresel[1]*, François-Xavier d'Abzac[1,2], Hugo Bucher[3], and Urs Schaltegger[1]
[1]Department of Earth Sciences, University of Geneva, Rue des Maraîchers 13, 1205 Geneva, Switzerland
[2]Geosciences Environnement Toulouse, Centre National de la Recherche Scientifique, l'Observatoire Midi-Pyrénées, Avenue Édouard Belin 14, 3100 Toulouse, France
[3]Paleontological Institute and Museum, University of Zurich, Karl Schmid-Strasse 4, 8006 Zurich, Switzerland

ABSTRACT

Accurate and precise dating of individual volcanogenic beds that spread across multiple sedimentary successions is a powerful tool to untangle stratigraphic age contradictions, since these horizons are deposited synchronously. In this study, we show that combining apatite chemistry with zircon age, Th/U ratio, and Hf isotope composition leads to reliable lateral correlation of volcanic horizons across sections representing disparate biological, chemical, and physical paleoenvironments. We correlate two volcanogenic horizons across six sedimentary sections straddling the Permian-Triassic boundary (PTB) in the Nanpanjiang Basin (South China), including the last Permian bed below the unconformity in shallow-water sections of the Luolou Platform. We place the PTB in our sections at the marked lithological change in order to avoid the difficulties that arise from the diachronism of the index conodont *Hindeodus parvus*, the first occurrence of which defines the PTB at the Global Stratotype Section and Point at Meishan. Our new data demonstrate that these volcanogenic beds are contemporaneous and cogenetic, allowing us to pool high-precision U-Pb zircon ages from the same horizon across several sections, and dating the last Permian volcanic event in this basin at 252.048 ± 0.033 Ma. We show that the mineral chemistry of apatite and zircon of intra- and interbasin-wide volcanogenic beds provides tie points against which biozones, carbon isotopes, astronomic cycles, and geomagnetic polarity time series can be stringently tested.

INTRODUCTION

Stratigraphic correlation of key sections, such as the Permian-Triassic boundary (PTB), usually rely on bio-, chemo-, magneto-, or cyclostratigraphic time series (e.g., Glen et al., 2009; Wu et al., 2013). Each of these approaches has limitations, which are largely inherent to *a priori* assumptions such as uniform sampling, completeness of the record through absence of local preservation effects, and synchronism and globalism of index species. The global definition and correlation of stage boundaries are usually based on the first occurrence (FO) of index species (e.g., Hillebrandt et al., 2013; Yin et al., 2001). Recently, Brosse et al. (2016) indicated that this approach leads to incorrect correlations for the PTB. Using biochronological methods based on graph theory (Guex et al., 2016), they revealed the diachronism of traditionally employed conodont interval zones, including the index species *Hindeodus parvus*, the FO of which defines the golden spike for the PTB at the base of Bed 27c in the Global Stratotype Section and Point (GSSP) at Meishan D. Hence,

other strategies have to be established in order to accurately correlate and calibrate key sequences in the stratigraphic record. U-Pb zircon chronology from volcanic horizons (e.g., Schoene et al., 2010; Burgess et al., 2014), also termed tephrochronology, allows temporal correlation of multiple sedimentary sections, across different paleoenvironments, independent from bio-, chemo-, or cyclostratigraphy. A prior assumption in tephrochronology has been that the age of zircon crystallization closely approximates that of the volcanic eruption and ash bed deposition (e.g., Bowring et al., 1998), and that the mineral age or chemistry is consistent across the entire ash horizon. Usually these assumptions are valid (see the discussion in Ovtcharova et al., 2015), and because tephra from volcanic eruptions can be transported over thousands of kilometers (e.g., Jensen et al., 2014), tephrochronology can provide an invaluable tool for stratigraphic correlation across entire sedimentary basins and beyond. The conventional practice in tephrochronology is to analyze the chemical composition of volcanogenic glass. This information is, however, likely to be biased by secondary alteration and devitrification, which can alter the original glass

composition (Cerling et al., 1985; McHenry, 2005), especially of pre-Cenozoic ashes. The chemistry of apatite and zircon offers a more robust tephrochronologic potential (e.g., Sell and Samson, 2011; Harvey, 2014; Nicklen et al., 2015), because they are ubiquitous in igneous systems and contain a large variety of non-stoichiometric elements. The partitioning of minor and trace elements (e.g., F, Cl, Fe, Mg, rare earth elements in apatite; e.g., Th, U, Hf in zircon) reflects the chemical composition of the magma from which they crystallized (e.g., Chazot et al., 1996; Nardi et al., 2013), and apatite and zircon are largely unaffected by chemical alteration during diagenesis (Morton and Hallsworth, 2007). Therefore, we utilized apatite and zircon chemistry as a tool to evaluate the cogenetic origin of volcanogenic beds, corroborated through high-precision U-Pb dating of zircon. This approach allows accurate stratigraphic correlation of volcanogenic beds between different sections straddling the PTB in marine successions of the Nanpanjiang Basin (Fig. 1A). Hence, we suggest placing the PTB at the ubiquitous marked lithological change, which differs from the FO of *H. parvus* in these sections (Fig. 1B). By this, we (1) demonstrate that our approach accurately defines individual horizons as synchronous stratigraphic tie points in the sedimentary record, and (2) offer an alternative definition of the PTB in the Nanpanjiang Basin, without utilizing the labile FO of *H. parvus*.

GEOLOGIC SETTING

The volcanogenic beds were sampled from six sections (Shanmenhai, Nanem, Wuzhuan, Tienbao, Penglaitan, and Dongpan) straddling the PTB in the Nanpanjiang Basin in southern China (Fig. 1A; for sample locations, see the GSA Data Repository[1]). During the Late Permian and
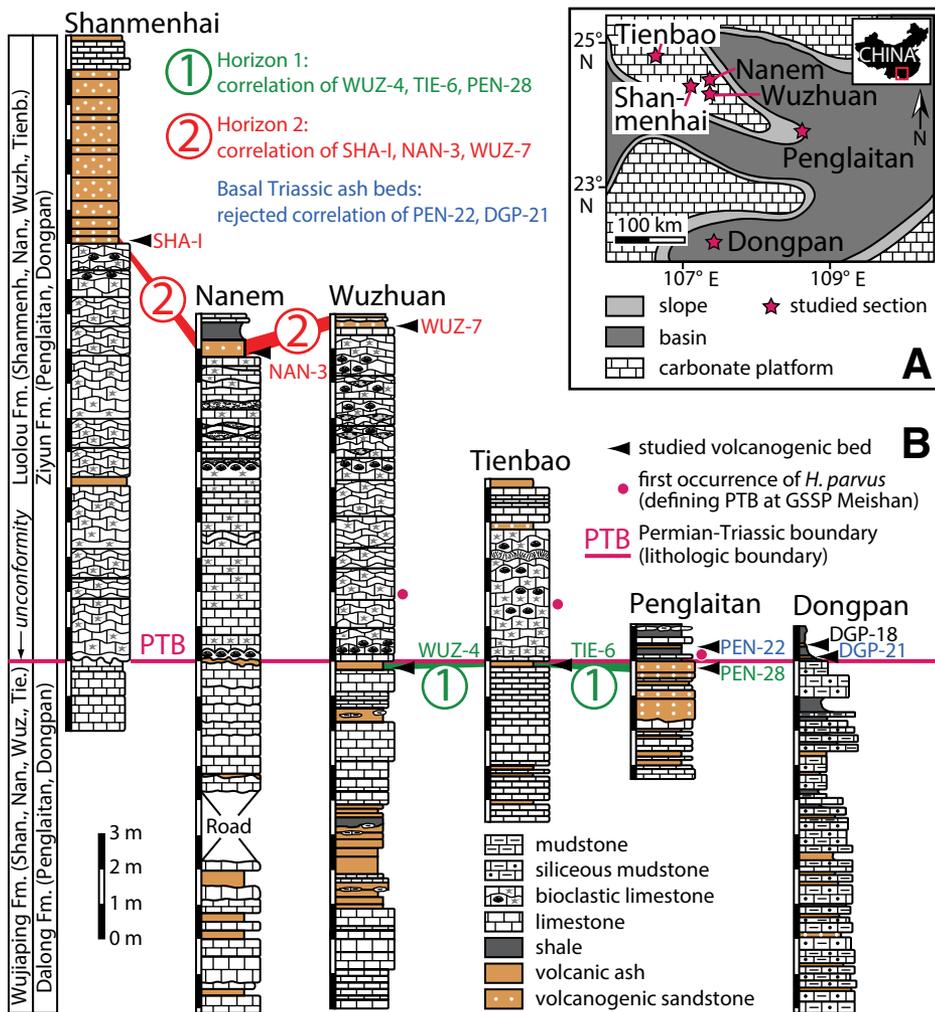
*E-mail: bjorn.baresel@unige.ch

Figure 1. A: Paleogeographic map of Nanpanjiang Basin (South China) showing positions of Shanmenhai, Nanem, Wuzhuan, and Tienbao shallow-marine platform sections, and of Penglaitan and Dongpan deeper-marine sections in Late Permian (modified after Wang and Jin, 2000). B: Lithostratigraphy of six studied sections including stratigraphic positions of investigated volcanogenic beds, first occurrence of *Hindeodus parvus*, and Permian-Triassic boundary (PTB). Stratigraphic correlation of volcanogenic horizons 1 and 2 is based on apatite chemistry and zircon U-Pb geochronology, Th/U ratios, and Hf isotopes. Ash beds PEN-22 and DGP-21 demonstrate advantage of our multiproxy approach, as evidenced in Figure 2C. GSSP—Global Stratotype Section and Point.

Early Triassic, this pull-apart basin was located on the present-day southern edge of the South China Block and occupied an equatorial position in the eastern Paleo-Tethys (Metcalfe, 2013). Volcanogenic beds are abundant in all sections; they are especially frequent in the deeper-water, low-energy settings of Penglaitan and Dongpan, and to a lesser degree in the shallow-water, higher-energy records of Shanmenhai, Nanem, Wuzhuan, and Tienbao (Fig. 1B). The volcanic material is presumably derived from the Lang Song volcanic arc, which is situated in the southwest part of the basin and was related to the convergence between Indochina and South China (Faure et al., 2016).

Late Permian rocks of the shallow-marine sections are assigned to the Wujiaping Formation and consist of limestones and subordinate volcanic ashes. Late Permian rocks of the deeper-water platform-slope sections belong to the Dalong Formation and consist of siliceous mudstones with subordinate limestones interbedded with abundant volcanic ashes and volcanogenic sandstones. Early Triassic rocks of the shallow-marine sections are assigned to the Luolou Formation, which rests unconformably on top of the Wujiaping Formation, whereas Early Triassic rocks of the deeper-water sections are assigned to the Ziyun Formation, which rests conformably on top of the Dalong Formation. The base of the Triassic is represented by microbialites in shallow-water settings and by laminated black shales in adjacent troughs. Therefore, the PTB in our sections is clearly and unambiguously expressed by these lithological boundaries (Fig. 1B).

SAMPLES AND ANALYTICAL METHODS

We report a comprehensive geochemical characterization of apatite by electron microprobe (EMP) analysis together with U-Pb high-precision, chemical abrasion–isotope dilution–thermal ionization mass spectrometry (CA-ID-TIMS) dates, Th/U ratios (obtained from ^{208}Pb/^{206}Pb TIMS analyses), and Hf isotopes (measured by multicollector–inductively coupled plasma–mass spectrometry) of zircon. Apatite and zircon were separated from nine volcanogenic beds covering the PTB interval in the Nanpanjiang Basin. The trace-element composition of 320 apatite crystals fingerprints each of these beds, and their temporal correlation is supported through 84 CA-ID-TIMS single-zircon U-Pb dates. This data set is complemented by Th/U ratios and Hf isotopes of the dated zircon crystals. Details of sampling, analytical methods, results, and reference material data are given in the Data Repository.

CORRELATING TEPHRA BEDS THROUGH APATITE AND ZIRCON CHEMISTRY

Analyzed apatites have equant to subequant crystal habits. This morphology usually reflects near-equilibrium crystallization conditions (Webster and Piccoli, 2015). Zircon crystals are predominantly long prismatic to acicular, presumably crystallizing at a late stage shortly before eruption. Fluorine concentrations ranging from 1.70 wt% to 4.07 wt% and a minor Cl component of 0.11 wt% to 0.87 wt% are typical of igneous apatite (Table DR3 in the Data Repository). Zircon yields Th/U ratios of 0.17–0.96 (Table DR4) and ε_{Hf} values of −12.9 to +0.9 (Table DR5), consistent with crystallization from SiO$_2$-rich melts of crustal origin, rather than an origin from the Siberian Traps, which has ε_{Hf} values of +4.8 to +16.3 (Malitch et al., 2010) and Th/U ratios of 1.00–2.67 (Burgess and Bowring, 2015). Studied ashes contain apatite and zircon with a unique chemical composition, which reflects the composition of the host magma at the time of eruption, providing a geochemical fingerprint for each volcanogenic bed in the Nanpanjiang Basin (Fig. 2; Figs. DR2–DR5). Among all volcanogenic beds investigated, two horizons can be unequivocally correlated around the PTB interval between several sections of the Nanpanjiang Basin (Fig. 1B).

Horizon 1—Uppermost Permian

Horizon 1 represents the last Permian bed characterized by volcanic ashes in the shallow-marine Luolou Platform at Wuzhuan (WUZ-4) and Tienbao (TIE-6), and by a volcanogenic sandstone in the deeper-marine section at Penglaitan (PEN-28). Apatites of Horizon 1 form two distinct populations in the Cl-MgO-FeO ternary plot and display similar chemistry and cathodoluminescence (CL; Fig. 2A; Fig. DR2). The cogenetic nature of the correlated beds is underlined by identical weighted mean ^{206}Pb/^{238}U ages from Wuzhuan (252.033 ± 0.067 Ma; N = 6; mean square of weighted
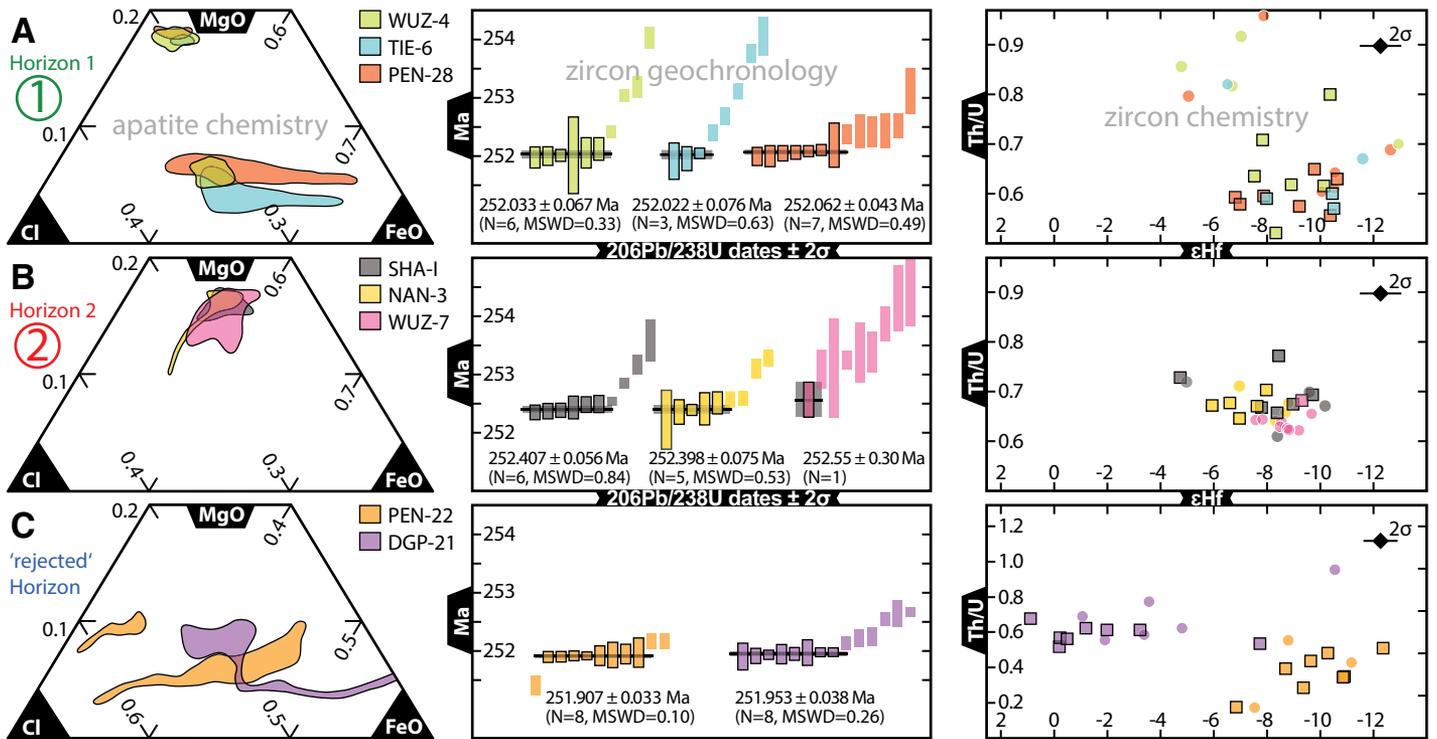
Figure 2. Apatite Cl-MgO-FeO ternary plots (each point is based on Cl, MgO and FeO concentrations in wt%, and represents the relative proportions of these three classes and always sum to 1), zircon U-Pb ages, and zircon Th/U versus ε_{Hf} plots for horizon 1 (A), horizon 2 (B), and "rejected" horizon (C). Data reveal equality of correlated volcanogenic beds pooled in both horizons shown in A and B. Note reduced scatter in Th/U and ε_{Hf} if only zircons defining weighted mean $^{206}Pb/^{238}U$ ages are considered (shown as squares). A: Correlation of last Permian bed (horizon 1) in Wuzhuan (WUZ-4), Tienbao (TIE-6), and Penglaitan (PEN-28). B: Correlation of Early Triassic volcanogenic sandstone bed (horizon 2), which marks top of microbial limestone in shallow-marine Shanmenhai (SHA-I), Nanem (NAN-3), and Wuzhuan (WUZ-7) sections. C: Necessity of our combined approach is demonstrated by zircon ages, which might reveal contemporaneity of basal Triassic ash beds in Penglaitan (PEN-22) and Dongpan (DGP-21), but apatite and zircon chemistry clearly refutes an identical origin. External reproducibility of Hf isotope analyses of 0.78 ε_{Hf} (2σ) corresponds to reproducibility of Plešovice reference zircon measurements (Table DR5; Fig. DR6 [see footnote 1]). Representative cathodoluminescence images of apatite from each volcanogenic bed are presented in Figures DR2–DR4. MSWD—mean square of weighted deviates.

deviates [MSWD] = 0.33), Tienbao (252.022 ± 0.076 Ma; N = 3; MSWD = 0.63), and Penglaitan (252.062 ± 0.043 Ma; N = 7; MSWD = 0.49; Fig. 2A). Dispersion of $^{206}Pb/^{238}U$ dates of up to 2 m.y. reveals incorporation of antecrystic zircon and/or sedimentary reworking as revealed by scattered zircon Th/U ratios and ε_{Hf} values. By removing these older grains, the overall variation in Th/U ratios and ε_{Hf} values reduces from 0.44 to 0.32 and from 8.1 units to 3.8 units, respectively (Fig. 2A). The overall variation of the youngest zircon clusters is identical in their Th/U ratios of 0.52–0.80 and their ε_{Hf} values of −10.6 to −6.8 (Fig. 2A). Apatite chemistry and zircon $^{206}Pb/^{238}U$ ages demonstrate that the volcanogenic beds assigned to horizon 1 are contemporaneous and cogenetic, rendering it a robust tie horizon in the Nanpanjiang Basin at the end of the Permian. At the Meishan GSSP (present-day northern margin of the South China Block), the last Permian volcanic bed (bed 25) has similar zircon chemistry, with Th/U ratios of 0.51–2.11 and ε_{Hf} values of −12.1 to −3.4 (He et al., 2014), but its weighted mean $^{206}Pb/^{238}U$ age of 251.941 ± 0.037 Ma (N = 16; MSWD = 1.3; Burgess et al., 2014) only coincides with Wuzhuan and Tienbao. The age difference with

Penglaitan can be potentially explained by the fact that it is a volcanogenic sandstone, not an ash layer.

Horizon 2—Early Triassic

Horizon 2 is represented by a volcanogenic sandstone in the shallow-marine sections of Shanmenhai (SHA-I), Nanem (NAN-3), and Wuzhuan (WUZ-7), and it accompanied the tectonic subsidence that drowned and consequently ended the growth of microbial limestone in the Nanpanjiang Basin. Its U-Pb ages of zircon are ~400 k.y. too old according to the computed model age of the PTB (Baresel et al., 2016) and thus violate the stratigraphic order. Nevertheless, the youngest grains or clusters are identical within uncertainty in the $^{206}Pb/^{238}U$ dates (Fig. 2B) from Shanmenhai (252.407 ± 0.056 Ma; N = 6; MSWD = 0.84), Nanem (252.398 ± 0.075 Ma; N = 5; MSWD = 0.53), and Wuzhuan (252.55 ± 0.30 Ma; youngest date). Apatite crystals define narrow overlapping clusters in the Cl-MgO-FeO ternary plot and show comparable CL (Fig. 2B; Fig. DR3). Zircon crystals display limited overlapping variations in their Th/U ratios and ε_{Hf} values (Fig. 2B). Apatite and zircon chemistry suggests a uniform magmatic source with no

significant sedimentary reworking. Its specific magmatic fingerprint was likely acquired during a period of enhanced crystallization in the magma reservoir ~400 k.y. prior to eruption, and the melt was erupted together with its crystal cargo. In the deeper-water section at Dongpan, a volcanogenic sandstone (DGP-18) shows identical zircon chemistry, but its different apatite chemistry does not support assignment to horizon 2 (Figs. DR3 and DR5).

Basal Triassic Ash Beds

Volcanic ash beds in Penglaitan (PEN-22) and Dongpan (DGP-21) occur 0.5 m and 0.1 m above the PTB, respectively. They show identical zircon dates, but they are different in their apatite and zircon chemistry (Fig. 2C; Fig. DR4). Thus, apatite and zircon chemistry reveals that these coeval ash beds are derived from different magmatic systems and are uncorrelated, demonstrating that the combined approach of accessory mineral chemistry and geochronology is essential. This fact points to the coexistence of different, contemporaneous volcanic sources with slightly different magma compositions in the Nanpanjiang Basin during the Early Triassic.

IMPLICATIONS

This study presents a novel application of apatite and zircon chemistry, together with high-precision zircon geochronology, as a multiproxy tool to precisely and accurately correlate individual volcanogenic horizons across different sedimentary facies and sections. As a first result, we are able to define two marker horizons and establish them as reliable stratigraphic tie points bracketing the PTB in the Nanpanjiang Basin. This allows us to constrain the PTB in different lithological facies, i.e., at the top of the shallow-marine Wujiaping Formation and the deeper-marine Dalong Formation at highest precision. Furthermore, given the cogenetic nature of the volcanogenic beds, zircon U-Pb dates from the topmost Permian bed in Wuzhuan, Tienbao, and Penglaitan can be pooled, and a weighted mean age of 252.048 ± 0.033 Ma ($N = 16$; MSWD = 0.46) can be calculated for the last ash bed before the PTB. Correlation with the ash of bed 25 in Meishan is probable, but not certain. Eventually, the combination of the multiproxy approach proposed here with the application of probabilistic statistics to create accurate age-depth models (as proposed in Baresel et al., 2016) will lead to a precise recognition of the PTB in different sedimentary environments at the 0.01% precision range for $^{206}Pb/^{238}U$ dates. This will be far superior to what can be achieved from analysis of the strongly condensed Meishan GSSP and should be considered as an essential complement to the GSSP definition. It will furthermore allow more accurate quantification of the diachronism of *H. parvus*, the index conodont that defines the base of the Triassic, and it will provide a stringent test for chemical and physical correlation methods. On a general level, the approach we suggest may lead to a higher degree of confidence in the definition of stage boundaries and the timing of important biological, physical, and chemical events in Earth's history.

REFERENCES CITED
Baresel, B., Bucher, H., Brosse, M., Cordey, F., Guodun, K., and Schaltegger, U., 2016, Precise age for the Permian-Triassic boundary in South China from high precision U-Pb geochronology and Bayesian age-depth modelling: Solid Earth Discussions, doi:10.5194/se-2016-145.

Bowring, S.A., Erwin, D.H., Jing, G.Y., Martin, M.W., Davidek, K., and Wang, W., 1998, U/Pb zircon geochronology and tempo of the end-Permian mass extinction: Science, v. 280, p. 1039–1045, doi:10.1126/science.280.5366.1039.

Brosse, M., Bucher, H., and Goudemand, N., 2016, Quantitative biochronology of the Permian-Triassic boundary in South China based on conodont unitary associations: Earth-Science Reviews, v. 155, p. 153–171, doi:10.1016/j.earscirev.2016.02.003.

Burgess, S.D., and Bowring, S.A., 2015, High-precision geochronology confirms voluminous magmatism before, during, and after Earth's most severe extinction: Science Advances, v. 1, p. e1500470, doi:10.1126/sciadv.1500470.

Burgess, S.D., Bowring, S.A., and Shen, S.Z., 2014, High-precision timeline for Earth's most severe extinction: Proceedings of the National Academy of Sciences of the United States of America, v. 111, p. 3316–3321, doi:10.1073/pnas.1317692111, (erratum available at doi:10.1073/pnas.1403228111).

Cerling, T.E., Brown, F.H., and Bowman, J.R., 1985, Low-temperature alteration of volcanic glass: Hydration, Na, K, ^{18}O and Ar mobility: Chemical Geology, v. 52, p. 281–293, doi:10.1016/0168-9622(85)90040-5.

Chazot, G., Menzies, M.A., and Harte, B., 1996, Determination of partition coefficients between apatite, clinopyroxene, amphibole, and melt in natural spinel lherzolites from Yemen: Implications for wet melting of lithospheric mantle: Geochimica et Cosmochimica Acta, v. 60, p. 423–437, doi:10.1016/0016-7037(95)00412-2.

Faure, M., Lin, W., Chu, Y., and Lepvrier, C., 2016, Triassic tectonics of the southern margin of the South China block: Comptes Rendus Geoscience, v. 348, p. 5–14, doi:10.1016/j.crte.2015.06.012.

Glen, J.M.G., Nomade, S., Lyons, J.J., Metcalfe, I., Mundil, R., and Renne, P.R., 2009, Magnetostratigraphic correlations of Permian–Triassic marine-to-terrestrial sections from China: Journal of Asian Earth Sciences, v. 36, p. 521–540, doi:10.1016/j.jseaes.2009.03.003.

Guex, J., Galster, F., and Hammer, Ø., 2016, Discrete Biochronological Time Scales: Cham, Switzerland, Springer International Publishing AG, 160 p., doi:10.1007/978-3-319-21326-2.

Harvey, J.C., 2014, Zircon age and oxygen isotopic correlations between Bouse Formation tephra and the Lawlor Tuff: Geosphere, v. 10, p. 221–232, doi:10.1130/GES00904.1.

He, B., Zhong, Y.-T., Xu, Y.-G., and Li, X.-H., 2014, Triggers of Permo-Triassic boundary mass extinction in South China: The Siberian Traps or Paleo-Tethys ignimbrite flare-up?: Lithos, v. 204, p. 258–267, doi:10.1016/j.lithos.2014.05.011.

Hillebrandt, A.V., et al., 2013, The global stratotype sections and point (GSSP) for the base of the Jurassic System at Kuhjoch (Karwendel Mountains, Northern Calcareous Alps, Tyrol, Austria): Episodes, v. 36, p. 162–198.

Jensen, B.J.L., et al., 2014, Transatlantic distribution of the Alaskan White River Ash: Geology, v. 42, p. 875–878, doi:10.1130/G35945.1.

Malitch, K.N., Belousova, E.A., Griffin, W.L., Badanina, I.Y., Pearson, N.J., Presnyakov, S.L., and Tuganova, E.V., 2010, Magmatic evolution of the ultramafic-mafic Kharaelakh intrusion (Siberian craton, Russia): Insights from trace-element,

U-Pb and Hf-isotope data on zircon: Contributions to Mineralogy and Petrology, v. 159, p. 753–768, doi:10.1007/s00410-009-0452-z.

McHenry, L.J., 2005, Phenocryst compositions as a tool for correlating fresh and altered tephra, Bed I, Olduvai Gorge, Tanzania: Stratigraphy, v. 2, p. 101–115.

Metcalfe, I., 2013, Gondwana dispersion and Asian accretion: Tectonic and palaeogeographic evolution of eastern Tethys: Journal of Asian Earth Sciences, v. 66, p. 1–33, doi:10.1016/j.jseaes.2012.12.020.

Morton, A.C., and Hallsworth, C., 2007, Stability of detrital heavy minerals during burial diagenesis, *in* Mange, M.A., and Wright, D.T., eds., Heavy Minerals in Use: Developments in Sedimentology: Amsterdam, Netherlands, Elsevier, v. 58, p. 215–245, doi:10.1016/S0070-4571(07)58007-6.

Nardi, L.V.S., Formoso, M.L.L., Müller, I.F., Fontana, E., Jarvis, K., and Lamarão, C., 2013, Zircon/rock partition coefficients of REEs, Y, Th, U, Nb, and Ta in granitic rocks: Uses for provenance and mineral exploration purposes: Chemical Geology, v. 335, p. 1–7, doi:10.1016/j.chemgeo.2012.10.043.

Nicklen, B.L., Bell, G.L., and Huff, W.D., 2015, A new shelf-to-basin timeline for the Middle Permian (Guadalupian) Capitan depositional system, west Texas and southeastern New Mexico, USA: Stratigraphy, v. 12, p. 109–122.

Ovtcharova, M., Goudemand, N., Hammer, O., Guodun, K., Cordey, F., Galfetti, T., Schaltegger, U., and Bucher, H., 2015, Developing a strategy for accurate definition of a geological boundary through radio-isotopic and biochronological dating: The Early–Middle Triassic boundary (South China): Earth-Science Reviews, v. 146, p. 65–76, doi:10.1016/j.earscirev.2015.03.006.

Schoene, B., Guex, J., Bartolini, A., Schaltegger, U., and Blackburn, T.J., 2010, Correlating the end-Triassic mass extinction and flood basalt volcanism at the 100 ka level: Geology, v. 38, p. 387–390, doi:10.1130/G30683.1.

Sell, B.K., and Samson, S.D., 2011, A tephrochronologic method based on apatite trace-element chemistry: Quaternary Research, v. 76, p. 157–166, doi:10.1016/j.yqres.2011.03.007.

Wang, Y., and Jin, Y., 2000, Permian palaeogeographic evolution of the Jiangnan Basin, South China: Palaeogeography, Palaeoclimatology, Palaeoecology, v. 160, p. 35–44, doi:10.1016/S0031-0182(00)00043-2.

Webster, J.D., and Piccoli, P.M., 2015, Magmatic apatite: A powerful, yet deceptive, mineral: Elements, v. 11, p. 177–182, doi:10.2113/gselements.11.3.177.

Wu, H., Zhang, S., Hinnov, L.A., Jiang, G., Feng, Q., Li, H., and Yang, T., 2013, Time-calibrated Milankovitch cycles for the Late Permian: Nature Communications, v. 4, p. 2452, doi:10.1038/ncomms3452.

Yin, H.F., Zhang, K.X., Tong, J.N., Yang, Z.Y., and Wu, S.B., 2001, The global stratotype section and point (GSSP) of the Permian-Triassic boundary: Episodes, v. 24, p. 102–114.